

Simplified Analysis of PWM Converters Using Model of PWM Switch Part I: Continuous Conduction Mode

VATCHÉ VORPÉRIAN

Virginia Polytechnic Institute and State University

A circuit-oriented approach to the analysis of pulsewidth modulation (PWM) converters is presented. This method relies on the identification of a three-terminal nonlinear device, called the PWM switch, which consists of only the active and passive switches in a PWM converter. Once the invariant properties of the PWM switch are determined, an average equivalent circuit model for it can be derived. This model is versatile enough that it can easily account for storage-time modulation of BJTs. The dc and small-signal characteristics of a large class of PWM converters can then be obtained by a simple substitution of the PWM switch with its equivalent circuit model. The methodology presented is very similar to linear amplifier circuit analysis whereby the transistor is replaced by its equivalent circuit model. Consequently, for the novice, this method should serve as a very smooth introduction to the analysis of PWM converters.

In this article the concept of the pulsewidth modulation (PWM) switch is introduced which leads to considerable simplification in the analysis (linear and nonlinear) and generation of dc-to-dc converters. To show the simplicity and elegance of the *PWM switch model* the dc and small-signal analysis of basic dc-to-dc converters is given. Of course, the results of the dc and small-signal analysis of dc-to-dc PWM converters are well known today from the *systematic* method of state-space averaging and its *canonical circuit model* [1, 2]. Hence, before going any further, a brief description of the two models mentioned above is given and the *difference* in the analytical approach between them is explained in order to justify the purpose of this article. First, the *canonical circuit model* completely represents the dc and small-signal characteristics of a PWM converter and is obtained after a considerable amount of matrix manipulations in order to single out the desirable input and output characteristics of the converter (input impedance, line-to-output transfer function, and output impedance) in addition to its control-to-output characteristics. The *PWM switch model*, on the other hand, represents only the dc and small-signal characteristics of the nonlinear part of the converter, which consists of the active and passive switches (the PWM switch), and is obtained after a few lines of very simple algebra. The dc and small-signal characteristics of a PWM converter are then obtained by replacing the PWM switch with its equivalent circuit model in a manner similar to obtaining the small-signal characteristics of linear amplifiers whereby the transistor is replaced by its equivalent circuit model. There are two advantages in using the model of the PWM switch. First, the PWM switch model allows many PWM converters to be analyzed using simple linear electronic circuit analysis programs (P-SPICE, MICRO-CAP to name a few), which allow for user-defined models (macros), without recourse to special-purpose programs which manipulate state-space equations. The second and more important advantage is a *pedagogical* one. More and more universities are beginning to teach power electronics at the senior level in their undergraduate program. Although students at this level are familiar with some matrix algebra, it would be far easier for them to learn all about the dc and small-signal properties of PWM converters using the method of *equivalent circuit model* which they learned in their electronics courses earlier. Students spend quite a bit of time learning about the nonlinear characteristics of the transistor and its small-signal equivalent circuit model. They later use this model to analyze the small-signal characteristics of linear amplifiers simply by replacing the transistor with its equivalent circuit model. Why not do the same in power electronics? Ultimately, whether or not the PWM switch model presented here is a useful

Manuscript received February 16, 1989; revised June 16, 1989.

IEEE Log No. 33463A.

Author's address: Virginia Power Electronics Center, Dep't. of Electrical Engineering, Virginia Polytechnic Institute and State University, Blacksburg, VA 24061.

0018-9251/90/0500-0490 \$1.00 © 1990 IEEE

educational tool depends on how well it is received by the educators in the field of power electronics.

The model of the PWM switch along with the model of the resonant switch were developed while work on the small-signal analysis of quasi-resonant converters was being conducted [3–6]. With a model of the PWM and resonant switches, the small-signal characteristics of quasi-resonant and PWM converters could be compared easily. The relationship of the PWM switch to the converter cell approach to the generation of converters has been discussed in [7], while a similar but more limited approach was given earlier in [11, 16]. Subsequently, the nonlinear analysis of the PWM switch was performed [9, 10] which resulted in considerable simplification over previous attempts namely, the perturbation series method [8], and the Volterra functional series method [14].

PWM SWITCH AND ITS INVARIANT PROPERTIES

The four familiar PWM converters are shown in Fig. 1 where the active and passive switches are lumped together in a single functional block called the PWM switch. This functional block represents the total nonlinearity in these converters and is shown as a three-terminal nonlinear device in Fig. 2. For obvious reasons, the terminal designations a, p, c refer to *active*, *passive*, and *common*, respectively. The voltage and current port designations of this device are important if we are to think of the PWM switch as the basic building block of the converters in Fig. 1. It can be seen that in each converter the external circuit elements are connected to the switch in such a way as to provide the proper port conditions given in Fig. 2. Hence, we see that the converters of Fig. 1 are obtained by a simple permutation of the PWM switch. A similar cyclic permutation of the PWM switch to generate some basic converters was discussed in [11] but its significance on the analysis of converters was never realized.

Next we investigate the *invariant* relationships between the terminal currents and voltages of the PWM switch which are shown in Fig. 3. It can be easily seen that the instantaneous current in the active terminal is always the same as the current in the common terminal during the on-interval DT_s no matter which configuration the switch is implemented in. Also, the instantaneous port voltages $\bar{v}_{cp}(t)$ and $\bar{v}_{ap}(t)$ are always coincident during DT_s . Hence, the invariant relations in the *instantaneous* terminal quantities are given by

$$\bar{i}_a(t) = \begin{cases} \bar{i}_c(t), & 0 \leq t \leq DT_s \\ 0, & DT_s \leq t \leq T_s \end{cases} \quad (1a)$$

$$\bar{v}_{cp}(t) = \begin{cases} \bar{v}_{ap}(t), & 0 \leq t \leq DT_s \\ 0, & DT_s \leq t \leq T_s \end{cases} \quad (1b)$$

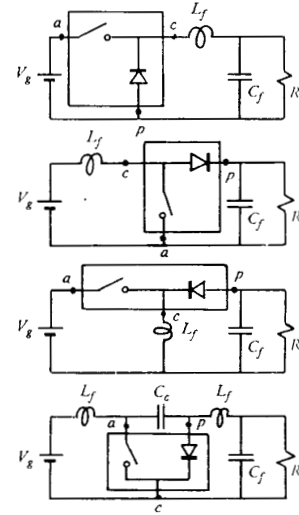


Fig. 1. Four basic PWM converters.

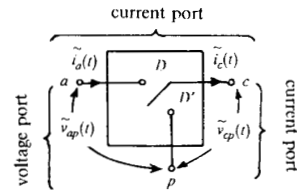


Fig. 2. PWM switch.

Since in dc-to-dc converters the behavior of the average quantities is of greater interest in determining the dc and small-signal characteristics of these converters, we seek to determine the *invariant* relationships between the *average* terminal quantities. Hence, for the *average* terminal currents i_a and i_c we have from very simple considerations

$$i_a = di_c \quad (2)$$

The instantaneous and average voltages across port $a-p$ require special attention. Since this port is a voltage port, it is connected either across a voltage source or a capacitor which in general has an ESR. Hence, the voltage waveform across this port consists in general of a small square wave (with a tilted top) riding on top of a large average value as shown in Fig. 3. The source of the square wave is the ESR of the capacitor which absorbs a pulsating current of peak-to-peak amplitude equal to the maximum value of the current in the common terminal. Hence, if the ESR of this capacitor is equal to zero, then the instantaneous voltage $\bar{v}_{ap}(t)$ is continuous and consists only of the capacitive ripple (which in the averaging process is neglected). Furthermore, this capacitor may be connected directly across terminals $a-p$ as in the case of the Cuk, boost, and buck with input filter converters, or indirectly as in the case of the

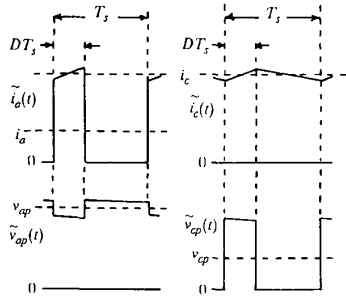


Fig. 3. Relation between terminal voltages and currents of PWM switch.

buck-boost converter. If we neglect the ripple in the common terminal current and consider only its average value i_c , then the peak-to-peak ripple voltage due to the ESR shown in Fig. 4 can be expressed as

$$v_r = i_c r_e \quad (3)$$

where r_e is in general a function of the ESR of the capacitor and the load resistor R . For example, in the boost and buck-boost converters the pulsating current of amplitude i_c is absorbed by the output filter capacitor which is in parallel with the output load resistor so that r_e is given by

$$r_e = r_{C_f} \parallel R, \quad \text{boost, buck-boost.} \quad (4a)$$

On the other hand, for the Cuk converter, we can see that

$$r_e = r_{C_c}, \quad \text{Cuk} \quad (4b)$$

because the peak-to-peak pulsating current ($i_c = i_{in} + i_0$) is absorbed only by the energy transfer capacitor and the square ripple is only due to its ESR. Hence, depending upon the converter, one can figure out easily r_e . Referring to Fig. 4 we can now easily see that the relation between the average port voltages is given by

$$v_{cp} = d(v_{ap} - i_c r_e d'), \quad d' = 1 - d. \quad (5)$$

The desired invariant relations of the PWM switch are given by (1) and (5) and are summarized below

$$i_a = di_c \quad (6a)$$

$$v_{cp} = d(v_{ap} - i_c r_e d') \quad (6b)$$

If the ESR of the capacitor, which absorbs the pulsating current, can be neglected then (6) reduce to

$$i_a = di_c \quad (7a)$$

$$v_{cp} = dv_{ap}. \quad (7b)$$

DC AND SMALL-SIGNAL MODEL OF PWM SWITCH

Let us first assume that the duty ratio is fixed at $d = D$ and that the terminal currents and voltages

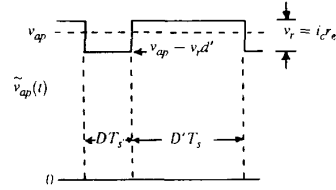


Fig. 4. Terminal voltage $\tilde{v}_{ap}(t)$ in presence of ESR of capacitor which absorbs pulsating current in converter.

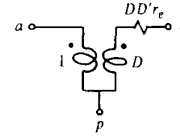


Fig. 5. Equivalent average circuit model of PWM switch for fixed duty ratio D .

of the PWM switch are perturbed because of some perturbation in either the input voltage or the load of the converter. Perturbing (6a) and (6b) for a fixed duty ratio, we get basically the same thing

$$\hat{i}_a = D\hat{i}_c \quad (8a)$$

$$\hat{v}_{cp} = D(\hat{v}_{ap} - \hat{i}_c r_e D'). \quad (8b)$$

These equations correspond to the model of the PWM switch for a fixed duty ratio as shown in Fig. 5 which is also valid all the way down to dc. Suppose we wanted to compute the open-loop line-to-output transfer function of a converter. The model to use then would be the one shown in Fig. 5 as is explained in the next section. If on the other hand, we would like to determine the response of the converter to perturbations in the duty ratio; we perturb (6a) and (6b) as follows

$$\hat{i}_a = D\hat{i}_c + I_c \hat{d} \quad (9a)$$

$$\hat{v}_{cp} = D(\hat{v}_{ap} + I_c r_e \hat{d} - \hat{i}_c r_e D') + \hat{d}(V_{ap} - I_c r_e D')$$

which can be rearranged as

$$\hat{v}_{ap} = \frac{\hat{v}_{cp}}{D} + \hat{i}_c r_e D' - [V_{ap} + I_c(D - D')r_e] \frac{\hat{d}}{D}. \quad (9b)$$

These equations correspond to the dc and small-signal model of the PWM switch shown in Fig. 6. Notice that if we neglect r_e , the model simplifies to the model shown in Fig. 7, which can also be obtained by perturbing (7a) and (7b). Equations (9a) and (9b) are summarized as follows:

$$\hat{i}_a = D\hat{i}_c + I_c \hat{d} \quad (10a)$$

$$\hat{v}_{ap} = \frac{\hat{v}_{cp}}{D} + \hat{i}_c r_e D' - V_D \frac{\hat{d}}{D} \quad (10b)$$

where

$$V_D = V_{ap} + I_c(D - D')r_e. \quad (10c)$$

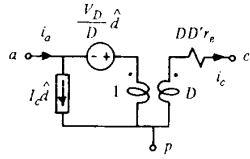


Fig. 6. Equivalent dc and small-signal model of PWM switch.

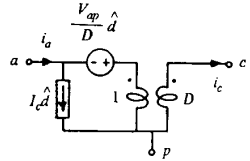


Fig. 7. Simplified dc and small-signal model of PWM switch.

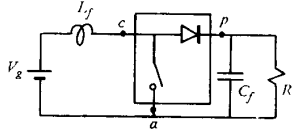


Fig. 8. Boost converter.

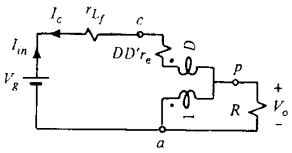


Fig. 9. Boost converter to be analyzed for dc characteristics using model of PWM switch shown in Fig. 5.

ANALYSIS OF PWM CONVERTERS USING MODEL OF PWM SWITCH

We now show how the model of the PWM switch is used to determine the dc as well as *all* the small-signal characteristics of PWM converters. The boost converter with all the parasitics shown in Fig. 8 is used as an example.

DC Analysis: Point-by-point substitution of the dc model of the PWM switch (Fig. 5) in the boost converter gives the circuit in Fig. 9 from which we can immediately determine the dc conversion ratio

$$M = \frac{V_0}{V_g} = \frac{1}{D'} \frac{1}{1 + \frac{r_{L_f}}{D'^2 R} + \frac{r_e D'}{R D'}} \quad (11)$$

where $r_e = r_{C_f} \parallel R$ as explained in (4a). The two other dc quantities which determine the operating point of the switch are I_c and V_{ap} . These are easily determined from Fig. 9

$$V_{ap} = -V_0 \quad (12a)$$

$$I_c = -I_{in} = -\frac{I_0}{D'}. \quad (12b)$$

Hence V_D can be calculated from (10c).

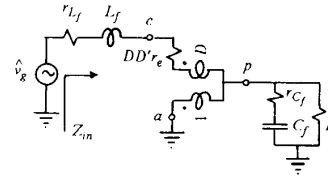


Fig. 10. Boost converter to be analyzed for line-to-output and input impedance functions using model of PWM switch shown in Fig. 5.

Open-Loop Line-to-Output Transfer Function: Under open-loop considerations the model in Fig. 5 still applies. Hence, to determine the line-to-output transfer the dc input voltage is replaced with a signal source \hat{v}_g as shown in Fig. 10 whence we can immediately determine

$$\frac{\hat{v}_0(s)}{\hat{v}_g(s)} = M \frac{(1 + s/s_{z1})}{1 + s/\omega_0 Q + s^2/\omega_0^2} \quad (13)$$

where

$$s_{z1} = \frac{1}{r_{C_f} C_f} \quad (14a)$$

$$\omega_0 = \frac{1}{\sqrt{L_f C_f}} \sqrt{\frac{r_{L_f} + r_e D D' + D'^2 R}{r_{C_f} + R}} \quad (14b)$$

$$Q = \frac{\omega_0}{\frac{r_{L_f} + r_e D'}{L_f} + \frac{1}{C_f (r_{C_f} + R)}} \quad (14c)$$

where $r_e = r_{C_f} \parallel R$ as discussed earlier in (4a).

Open-Loop Input Impedance: From Fig. 10 we can continue to determine the input impedance

$$Z_{in} = R_{in} \frac{1 + s/\omega_0 Q + s^2/\omega_0^2}{1 + s/s_p} \quad (15)$$

where

$$R_{in} = r_{L_f} + r_e D D' + D'^2 R \quad (16a)$$

$$s_p = \frac{1}{C_f (r_{C_f} + R)}. \quad (16b)$$

The denominator is (of course) the same as in (13) and ω_0 and Q are given by (14b) and (14c).

Open-Loop Output Impedance: In this case we short the input to ground and connect a test voltage source at the output as shown in Fig. 11 and obtain

$$Z_0 = R_0 \frac{(1 + s/s_{z1})(1 + s/s_{z0})}{1 + s/\omega_0 Q + s^2/\omega_0^2} \quad (17)$$

where

$$R_0 = R \parallel \frac{r_{L_f} + r_e D D'}{D'^2} \quad (18a)$$

$$s_{z0} = \frac{r_{L_f} + r_e D D'}{L_f}. \quad (18b)$$

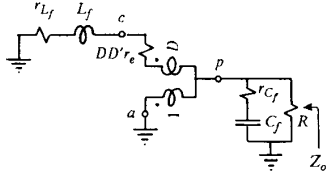


Fig. 11. Boost converter to be analyzed for output impedance function using model of PWM switch shown in Fig. 5.

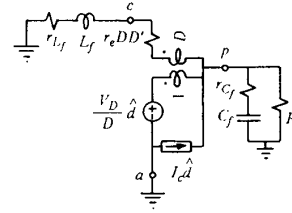


Fig. 12. Boost converter to be analyzed for control-to-output transfer function using model of PWM switch shown in Fig. 6.

The quadratic in the denominator is the same as in (13) and s_{z1} is the same as in (14a).

Control-to-Output Transfer Function: In this case the input voltage source V_g is shorted to ground and the PWM switch is replaced by its equivalent circuit model of Fig. 6 as shown in Fig. 12. Although one can directly determine the control-to-output transfer function in a straightforward manner from Fig. 12, we can take some short cuts and use some tricks of network analysis [15]. Hence, we expect the denominator of the control-to-output transfer function to be the same as that of the line-to-output transfer function as given in (13) so that we have

$$\frac{\hat{v}_0(s)}{\hat{d}(s)} = K_d \frac{(1 + s/s_{z1})(1 - s/s_{z2})}{1 + s/\omega_0 Q + s^2/\omega_0^2} \quad (19)$$

where ω_0 and Q are given by (14b) and (14c). The low frequency asymptote K_d is simply given by

$$K_d = \frac{dV_0}{dD} = V_g \frac{dM}{dD} \approx \frac{V_g}{D^2} \quad (20)$$

as can be easily verified from (11). All that remains to be determined is the numerator in (19) which corresponds to the zeros or the *nulls* of the output voltage. To determine these zeros we simply consider the circuit of Fig. 12 under null conditions of the output, i.e., $v_0(s_{z2}) = 0$ and $v_0(-s_{z1}) = 0$. The transform circuit under null conditions of the output is shown in Fig. 13. The first null is determined by the zero of the impedance of the output filter which is simply given by

$$r_{C_f} + \frac{1}{sC_f} \Big|_{s=-s_{z1}} = 0 \rightarrow s_{z1} = \frac{1}{r_{C_f} C_f}. \quad (21)$$

The second null in the output voltage is given by the null in the passive terminal current, i.e., $\hat{i}_p(s_{z2}) = 0$. For the second null we see that the control generator $V_D \hat{d}/D$ appears across the transformer whose secondary voltage appears across r_{L_f} , $r_e DD'$ and L_f . Hence we have

$$\frac{\hat{d}V_D}{D} D = \hat{i}_c (r_{L_f} + r_e DD' + s_{z2} L_f) \quad (22)$$

where $r_e = r_{C_f} \parallel R$ as discussed earlier in (4a). Also, at the active terminal junction we have

$$\hat{i}_c = I_c \hat{d} + \hat{i}_c D. \quad (23)$$

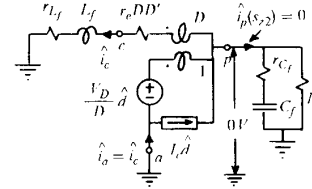


Fig. 13. Determination of zeros, or nulls, of control-to-output transfer function.

Solving (22) and (23) we get

$$s_{z2} = \frac{1}{L_f} \left(D' \frac{V_D}{I_c} - r_{L_f} - r_e DD' \right). \quad (24)$$

Finally, use of the operating point, (V_D, I_c) , determined in (12a) and (12b) in (24) gives

$$s_{z2} = \frac{D'^2}{L_f} (R - r_{C_f} \parallel R) - \frac{r_{L_f}}{L_f}. \quad (25)$$

Hence, the control-to-output transfer function has been completely determined.

MODEL OF PWM SWITCH INCLUDING STORAGE-TIME MODULATION

The model of the PWM switch is versatile enough to include parasitic effects such as storage-time modulation which Middlebrook has described in [12]. The effect of storage-time modulation in BJTs can be accounted for by a simple change in the perturbation of the duty ratio as follows

$$\hat{d} \rightarrow \hat{d} - \frac{\hat{i}_c}{I_{me}} \quad (26)$$

where I_{me} is a modulation parameter which depends on the type of base drive (proportional, direct, etc.) as discussed in [13]. Substitution of the above in (10a)–(10c) gives

$$\hat{i}_a = \left(D - \frac{I_c}{I_{me}} \right) \hat{i}_c + I_c \hat{d} \quad (27)$$

$$\hat{v}_{ap} = \frac{\hat{v}_{cp}}{D} + \hat{i}_c \left(r_e D' + \frac{r_m}{D} \right) - \frac{V_D}{D} \hat{d} \quad (28)$$

where

$$r_m = \frac{V_D}{I_{me}} \equiv \text{modulation resistance}. \quad (29)$$

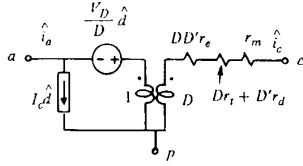


Fig. 14. Equivalent circuit model of PWM switch including effects of storage-time modulation and resistances of diode and transistor branches. Under dc conditions, nondissipative modulation resistance r_m disappears.

According to the approximations explained in [12 and 13], $D \gg I_c/I_{me}$ so that (27) reduces to its original form. With this approximation, the above equations correspond to a simple modification in the model of the PWM switch shown in Fig. 14 where a *nondissipative* modulation resistance r_m has been added in series with the common terminal.

Other parasitic elements such as the lead resistances in the active and passive switches shown in Fig. 15, can be easily included in the switch model without much difficulty. Intuitively, it can be seen from Fig. 15 that the common terminal spends D -percent of its time in series with r_t and D' -percent of its time in series with r_d so that the total effective resistance in the common terminal must be $Dr_t + D'r_d$ as shown in Fig. 14. This can be verified formally if we write the correct relationship between the average terminal voltages (as we did in (5)) in the presence of r_t and r_d as

$$v_{cp} = d(v_{ap} - i_c r_e d' - e_c r_t) - d' i_c r_d. \quad (30)$$

If this equation is perturbed, our intuitive derivation is confirmed with a minor adjustment in V_D

$$V_D = v_{ap} + (D - D')I_c r_e + I_c(r_d - r_t). \quad (31)$$

Almost always one can use the approximation $V_D \simeq V_{ap}$ as can be seen from the above. The equations corresponding to the model of the PWM switch in Fig. 14 including all the parasitic effects, are summarized below

$$\hat{i}_a \simeq D\hat{i}_c + I_c\hat{d} \quad (32a)$$

$$\hat{v}_{ap} = \frac{\hat{v}_{cp}}{D} + \hat{i}_c r_c - \frac{V_D}{D}\hat{d} \quad (32b)$$

where

$$r_c = r_m + Dr_t + D'r_d + DD'r_e \quad (32c)$$

$$V_D = v_{ap} + (D - D')I_c r_e + I_c(r_d - r_t). \quad (32d)$$

As a final example we consider the line-to-output transfer function of the Cuk converter including all the parasitic elements as discussed in [13]. Researchers in the early days of this converter were puzzled with the peculiar behavior in the phase response of the line-to-output transfer function which at higher frequencies showed a variation from -90 to 90 degrees. Since a similar behavior in the

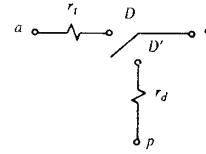


Fig. 15. PWM switch showing resistances of transistor and diode branches.

control-to-output transfer function was not observed, it was immediately suspected that the culprit was the numerator in the line-to-output transfer function. The converter was first modeled including all the parasitic elements of the passive components assuming ideal switches, but no anomalous behavior in the phase response was seen. Finally, when the modulation resistance and the resistances of the diode and the transistor branches were included, a new zero was discovered which could move anywhere from the left-half plane to the right-half plane depending upon the values of r_m (which can be made positive or negative), r_d , and r_t . In order to appreciate the model of the PWM switch, one should go through the method of state-space averaging and its canonical circuit model employed in [13] and compare it with the method given below using the model of the PWM switch which yields the same desired results almost by *inspection*. Thus, the model of the PWM switch in Fig. 14, without the control sources, is substituted in the Cuk converter as shown in Fig. 16 to determine the open-loop line-to-output transfer function. Since we are interested here only in the numerator, we study this circuit in the transform domain under null conditions of the output. The first null is clearly given by the null of the impedance of the output filter as in (21). The second null is given by the null in the inductor current $\hat{i}_{L_2}(s) = 0$. For this second null we can immediately see from Fig. 16 that

$$\hat{i}_c r_c \frac{1}{D} = (\hat{i}_c - D\hat{i}_c) \left(r_c + \frac{1}{sC_c} \right) \quad (33)$$

which can be immediately solved for s to give the second zero

$$s_{z2} = \frac{1}{C_c \left(\frac{r_c}{DD'} - r_c \right)}. \quad (34)$$

Recalling r_c from (32c) and $r_e = r_c$ from (4b) we get from (34)

$$s_{z2} = \frac{DD'}{C_c(Dr_t + D'r_d + r_m)} \quad (35)$$

where

$$r_m = \frac{V_D}{I_{me}} \simeq \frac{V_{ap}}{I_{me}} = \frac{(V_0 + V_g)}{I_{me}} = \frac{V_0}{DI_{me}} \quad (36)$$

where we have made use of the fact that for the Cuk converter $V_0/V_g = D/D'$. Hence, the numerator of the

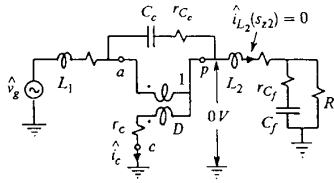


Fig. 16. Cuk converter, including all parasitic elements, to be analyzed for audio. Null condition corresponding to second zero of audio transfer function is shown.

line-to-output transfer function can now be written as

$$\frac{\hat{v}_0(s)}{\hat{v}_g(s)} = M \frac{(1 + s/s_{z1})(1 - s/s_{z2})}{D(s)} \quad (37)$$

where s_{z1} and s_{z2} are determined above in (21) and (35), respectively, and $D(s)$ is a fourth-order polynomial. It is this second zero s_{z2} which is entirely dependent on the parasitic resistances of the switches that causes variations in the high end of the phase response. It has been shown in [13] that r_m can be easily made sufficiently negative that the zero can migrate from the right-half plane to the left-half plane resulting in variations from -90 to 90 degrees at the high end of the phase response.

CONCLUSIONS

A new, simple, and circuit-oriented method of analysis of PWM converters, which uses the model of the PWM switch developed in this article, is presented. In this method, the model of the PWM switch is used in the same way as the model of the transistor is used in the analysis of electronic amplifier circuits. The PWM switch is presented as a three-terminal nonlinear device which represents the total nonlinearity in a PWM converter just as the transistor represents the total nonlinearity in an electronic amplifier. Hence, as one does not linearize the entire equations of an amplifier along with the Ebers-Moll equations of the transistor to determine its dc and small-signal characteristics, one does not need to linearize the entire equations of a PWM converter as is done in the case of state-space averaging, circuit averaging or hybrid modeling.

Finally, with a model of the PWM switch PWM converters can be easily analyzed for dc and small-signal characteristics on standard electronic circuit analysis programs in closed-loop operation without the need for special-purpose programs.

REFERENCES

[1] Cuk, S. (1976)
Modelling, analysis and design of switching converters.
Ph.D. dissertation, California Institute of Technology,
Pasadena, Nov. 1976.

[2] Middlebrook, R. D., and Cuk, S. (1976)
A general unified approach to modelling
switching-converter power stages.
In *IEEE Power Electronics Specialists Conference
Proceedings*, 1976.

[3] Vorperian, V. (1986)
Average model of the single-pole double throw switch in
PWM converters.
Internal correspondence, Feb. 11, 1986.

[4] Vorperian, V., Tymerski, R., Liu, K., and Lee, F. C. (1986)
Generalized resonant switches: part I.
In *1986 VPEC Conference Proceedings*.

[5] Vorperian, V., Tymerski, R., Liu, K., and Lee, F. C. (1986)
Generalized resonant switches: part II.
In *1986 VPEC Conference Proceedings*.

[6] Vorperian, V. (1986)
Equivalent circuit models for PWM and resonant switches.
In *Proceedings of 1986 Conference International Symposium
or Circuits and Systems*, 3.

[7] Tymerski, R., and Vorperian, V. (1986)
Generation, classification and analysis of switched-mode
dc-to-dc converters by the use of converter cells.
INTELEC Conference Proceedings, 1986.

[8] Erickson, R. W. (1982)
Large signals in switching converters.
Ph.D. dissertation, California Institute of Technology,
Pasadena, Nov. 1982.

[9] Tymerski, R., Vorperian, V., Baumann, W., and Lee, F. C.
Nonlinear modeling of the PWM switch.
Accepted for publication, to appear in the *IEEE Journal of
Power Electronics*.

[10] Tymerski, R. (1988)
Topology and analysis in power conversion and inversion
circuits.
Ph.D. dissertation, Virginia Polytechnic Institute and State
University, Blacksburg, VA, May 1988.

[11] Cuk, S. (1977)
A new optimum topology switching dc-to-dc converter.
In *IEEE Power Electronics Specialists Conference
Proceedings*, 1977.

[12] Middlebrook, R. D. (1975)
A continuous model of the tapped boost converter.
In *IEEE Power Electronics Specialists Conference
Proceedings*, 1975.

[13] Polivka, W., Chetty, P., and Middlebrook, R. (1980)
State-space average modelling of converters with parasitics
and storage-time modulation.
In *IEEE Power Electronics Specialists Conference
Proceedings*, 1980.

[14] Tymerski, R. (1985)
The large signal forced response of switching amplifiers
using the Volterra functional series expansion.
Technical note T173, Power Electronics Group, Caltech,
Pasadena, CA, Apr. 1985.

[15] Vorperian, V.
Circuit-oriented analysis of PWM converters using the
model of PWM switch.
These are examples worked out in detail using many
tricks of network analysis. Available from the author upon
request.

[16] Landsman, E. E. (1979)
A unifying derivation of switching dc-dc converter
topologies.
In *IEEE Power Electronics Specialists Conference
Proceedings*, 1979, 239-243.

Author's photograph and biography will be found on
page 505 of this issue following Part II of this article.